

Figure1.



Figure2.

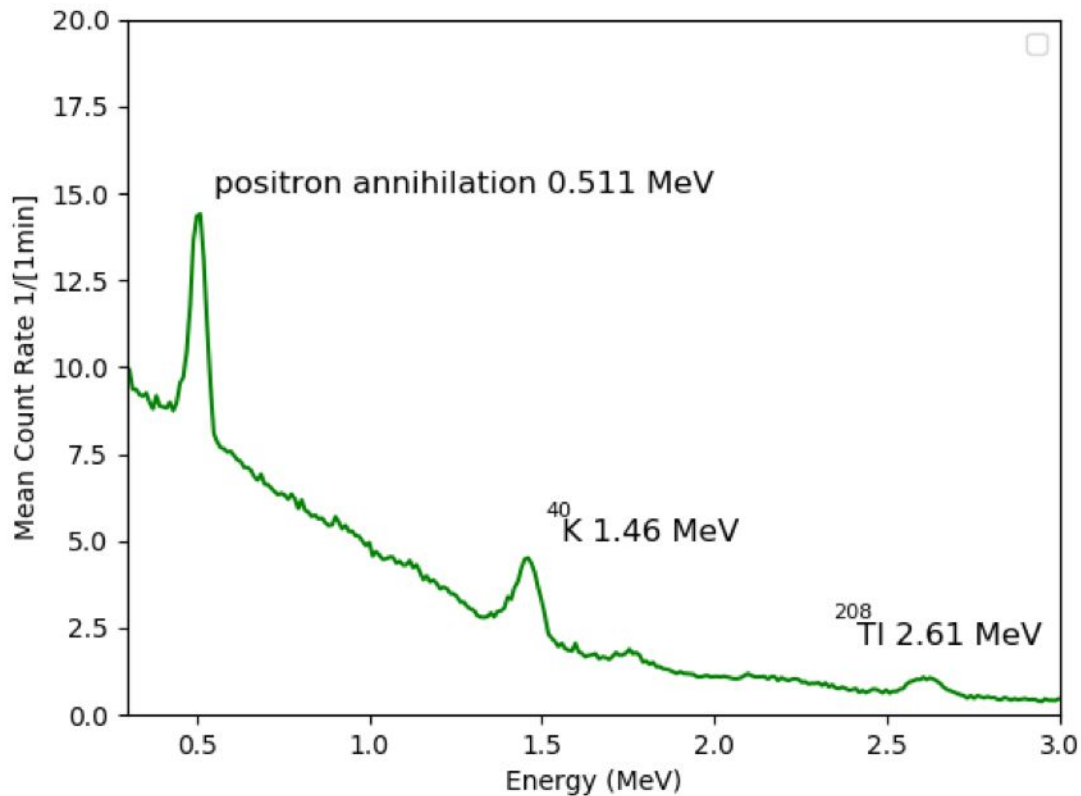


Figure3.

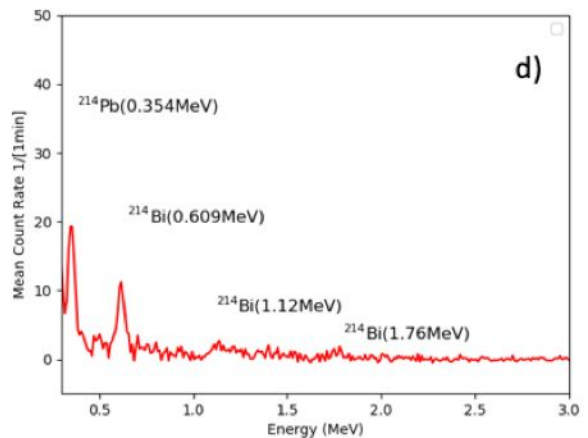
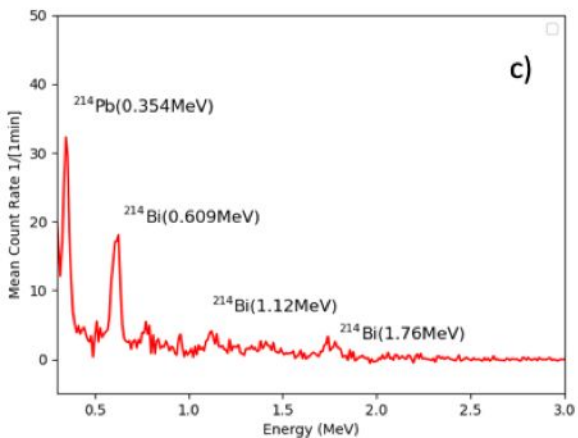
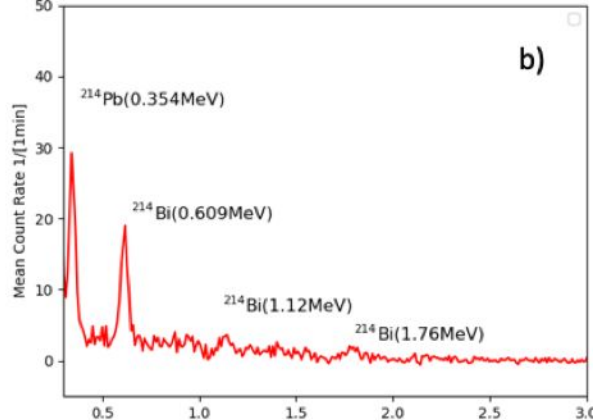
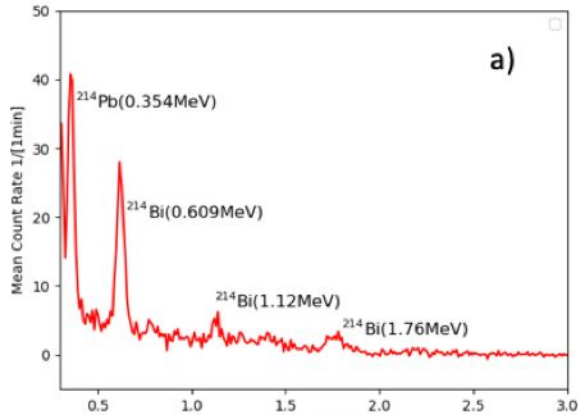
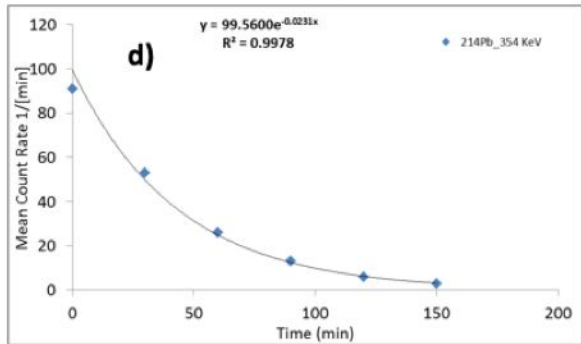
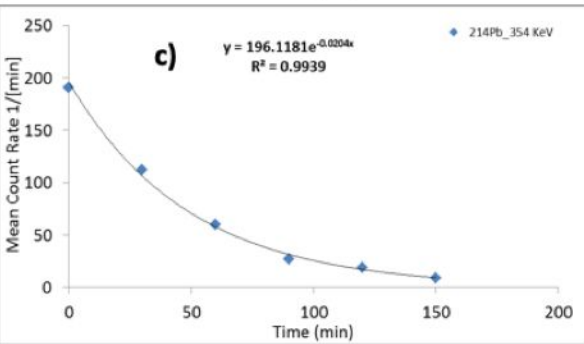
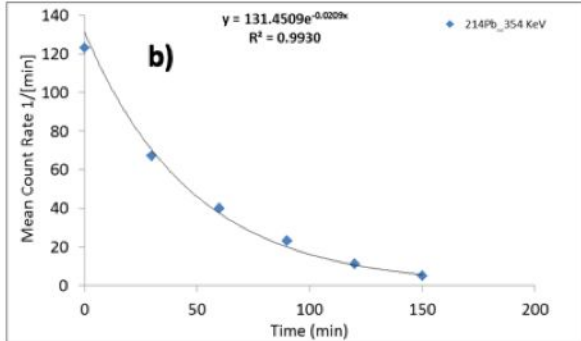
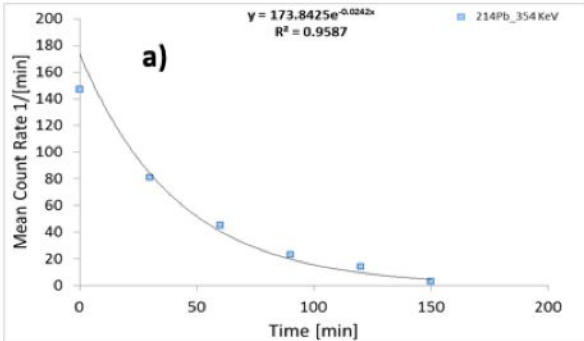


Figure4.



Circulation of Radon progeny in the terrestrial atmosphere during thunderstorms

A. Chilingarian^{1,2}, G. Hovsepyan¹, B. Sargsyan¹

¹A. Alikhanyan National Lab (Yerevan Physics Institute), Yerevan 0036, Armenia

²National Research Nuclear University MEPhI, Moscow 115409, Russia

Abstract

We describe a new phenomenon in atmospheric physics – ²²²Rn progeny circulation during thunderstorms. The enhancement of the natural gamma radiation during thunderstorms was measured with precise gamma ray spectrometers. Results of measurements performed at Aragats mountain in Armenia during summer 2020 demonstrate the Rn progeny lifted to the atmosphere by a near-surface electric field are returned backward to the ground by rain precipitation. Thus, thunderstorms not only return negative charge to the Earth by lightning flashes but, also maintain Rn progeny circulation in the atmosphere; it this way, significantly enlarging natural gamma radiation above the Earth surface and Radon concentration in the atmosphere.

1. Introduction

The terrestrial atmosphere is host to various sources of electric currents and gamma radiation ranging from the fair-weather current of picoamperes to hundreds of kiloampere lightning currents. Particle fluxes range from the single particles of the ambient population of secondary cosmic rays to huge particle showers from interactions of primary high-energy proton or nuclei with terrestrial atmosphere and electron-gamma ray avalanches from the electron accelerator operated in the thundercloud. Gamma radiation from the primordial radionuclides have the half-life comparable with the age of the Earth, and they contribute significantly to natural gamma radiation (NGR) at considerably low energies (<3MeV).

Radionuclides derived from the Earth crust can influence the electrical properties of the atmosphere and can influence human illness and death rates, result in DNA alterations, and chromosomal aberrations and weakening of immunity (Hunting et al., 2020).

The static electric field in the lower atmosphere is modulated by the mobile particles carrying electrical charges, i.e. different types of hydrometeors, aerosols, small ions, and progeny of radioactive isotopes. The charge separation initiated by the updraft of moisture generates an electric field between differently charged layers emerging in the thundercloud; potential drop (voltage) in the cloud can reach hundreds of megavolts. Emerging near-surface electric field lifts charged aerosols with attached ²²²Rn isotope and its progeny to the atmosphere. Correspondingly, the concentration of ²²²Rn at surface decreases 10 times (Wilkning et al., 1966, Roffman, 1972); the small ions and aerosols with attached ²²²Rn are lifted up in seconds to tens of meters due to their large mobility. These gamma emitters significantly enhance low-energy natural gamma radiation measured by spectrometers located several meters above the ground (Chilingarian, 2018, Chilingarian et al., 2019a, Chilingarian et al., 2019b). The rain returns long-lived progeny to the Earth recovering and somewhat enhancing

the surface radiation (washout process, McCarthy and Parks, 1992, Barbosa et al., 2017, Fabro et al., 2016), Reuveni et al., 2017, Chilingarian et al., 2020).

We present the measurement of the gamma radiation performed on Aragats mountain, 3200 m above sea level during summer thunderstorms. We estimate the intensity of the different ^{222}Rn progenies in the rainwater; clarify the washout process and estimate the percentage of isotopes returned by the rain to the Earth surface. For measurements, we use the precise ORTEC firm gamma spectrometer (NaI(Tl), FWHM $\sim 7.7\%$ at 0.6 MeV, see details in Hossain et al., 2012) surrounded with lead filters. Simulations of the cosmic radiation, radon progeny radiation, and detector response function calculation were performed with the aid of the EXPACS code (Sato, 2018).

2. Method

Gamma radiation measured on the Earth surface comes from the ground and from the atmosphere. The largest surface contribution is from gamma rays originating in the mineral grain, in their crystal lattices, and in the construction materials. The radiation is stable because the concentration of radionuclides in minerals and construction materials is constant due to long half-lives of their parent isotopes (^{40}K , ^{238}U , ^{232}Th , see details in (Chilingarian et al., 2019a). Therefore, to investigate Radon progeny circulation (lifted by the near-surface electric field and returned through precipitation from rain) in the atmosphere we need to take into account and filter as much as possible this more-or-less stable contribution of the radionuclides from the surface. Gamma spectrometers are positioned on Aragats in the experimental hall which is 3 meters high and located under a metallic tilt roof of 0.6 mm thickness. By surrounding the ORTEC spectrometer with the 4-cm thick lead filter (see Fig. 1) we suppress the Radon progeny gamma radiation ≈ 12 times; the count rate of the spectrometer decreases from 12600 ± 112 to 1080 ± 34 .



68

69 **Figure 1. ORTEC firm gamma spectrometer (NaI(Tl), FWHM $\sim 7.7\%$ at 0.6 MeV, see**
 70 **details in (Hossain et al., 2012), surrounded by 4 cm thick lead filters. The spectrometer**
 71 **is positioned in the experimental hall on Mt Aragats (3200 m MSL) which is 3 meters**
 72 **high and located under a metallic tilt roof of 0.6 mm thickness.**

73 In Fig. 2 we show the energy spectrum measured by ORTEC spectrometer for 6 hours
 74 (normalized to 1-minute count rate). Most pronounced are the positron annihilation peak (0.
 75 511 MeV), 40K peak (1.46 MeV), and 208Tl peak (2.61 MeV). Bismuth isotopes also are
 76 present in smaller quantities, see Table 1.

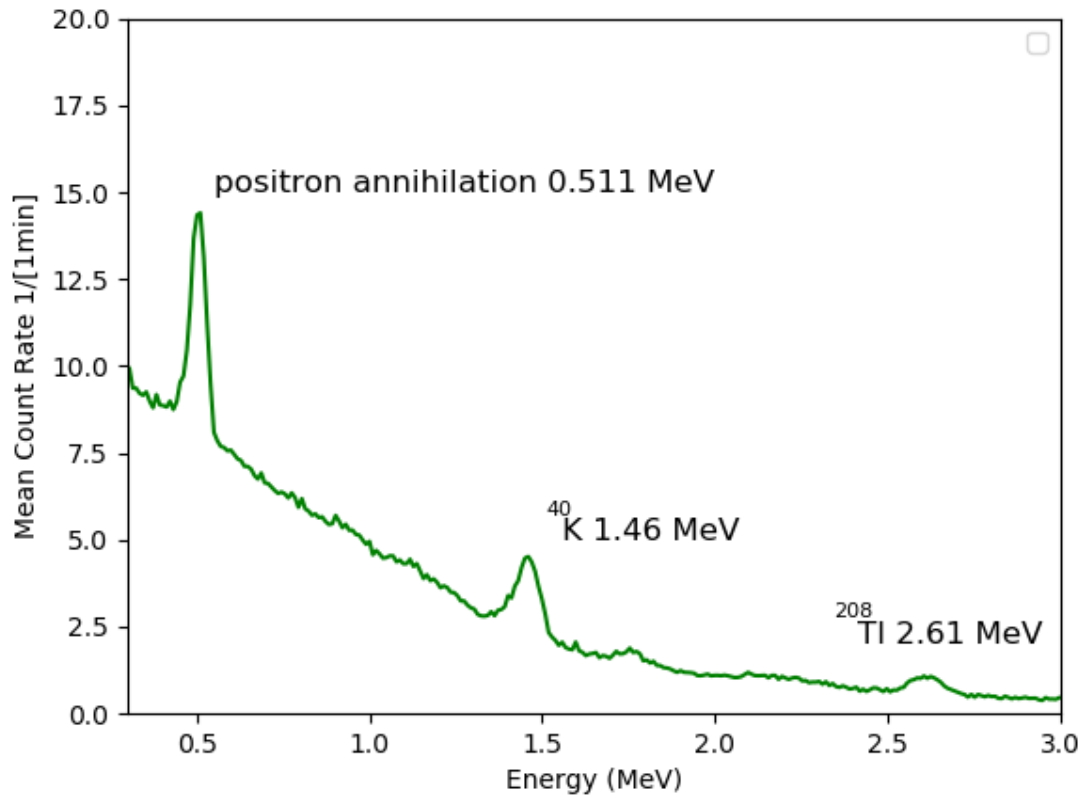


Figure 2. Energy spectra of the background measured by the ORTEC spectrometer surrounded by lead filter.

In the first column of Table I, we present the count rate of registered particles normalized to a 1-minute time span. Next is the absolute enhancement and its share of important isotopes from radon and thoron chains, potassium isotope peak, the 511 keV positron annihilation line, as well a small amount Cs-137 trace due to contamination of the ORTEC spectrometer during calibration with Cs isotope. In the last column, we show the overwhelming portion of the continuous spectrum induced by the secondary cosmic rays (CR) and Compton scattering of the gamma rays in the body of the NaI(Tl) crystal of ORTEC spectrometer.

Table 1. Composition of the background gamma radiation measured by ORTEC spectrometer surrounded from all sides by the 4-cm thick lead filter

Total intensity 0.3 -3 MeV	²¹⁴ Pb_354 keV	⁵¹¹ keV	¹³⁷ Cs 662 keV	²¹⁴ Bi 768 keV	²²⁸ Ac 911keV	²¹⁴ Bi 1.12 MeV	²¹⁴ Bi 1.76 MeV	²¹⁴ Bi 2.2 MeV	⁴⁰ K 1.46MeV	²⁰⁸ Tl 2.6 MeV	CR and Compton scattered
912	8	31	2	4	4	3	3	3	22	4	828
100%	0.9	3.4	0.2	0.4	0.4	0.3	0.3	0.3	2.4	0.4	90.8

To measure the share of Rn progeny in the rainwater we should subtract the background spectrum from the spectrum measured during exposing rainwater to the spectrometer (see details of technique in (Chilingarian et al., 2019b)). As we see in the last column of Table 1, the lead filter suppresses background down to a few percent; more than 90% of the count rate comes from the stable flux of high-energy cosmic rays penetrating the lead filter. Simulations of the detector response function with cosmic radiation, radon progeny radiation, were performed with EXPACS code (Sato, 2018) and coincide rather well with the experimentally measured count rate.

3. Results

In 2020 the first rain on Aragats was in June and rain showers were only during July, which is when they fille special container in a few minutes. In Fig. 3 we show four episodes of the radiation measurements (after subtracting the background). In Table 2 we show the count rates of gamma emitters including radioactive isotopes, positron annihilation, and continuous spectrum of secondary cosmic rays (mostly muons) and gamma rays scattered in the body of the NaI crystal (continuum to the right of each spectral line).

As it was expected from previous measurements the most pronounced peaks are ²¹⁴Pb and ²¹⁴Bi (Chilingarian et al., 2019c, Chilingarian et al., 2019b, Chilingarian et al., 2020), and as we show in Table 2 the share of different gamma-emitting isotopes in the atmosphere measured by the same spectrometer well coincides with the spectra measured from the rainwater (see Table 2 in Chilingarian et al, 2020). Sure, the electrified atmosphere introduces changes in the particle fluxes and slightly enlarges the positron annihilation share (see Fig. 6 in Livesay et al., 2014); however, these changes are not large and do not exceed $\approx 1\%$. The potassium spectrum is very stable and does not influence the rainwater spectrum. In the last row of Table 2, we show the mean value of each gamma emitter share and error of the mean.

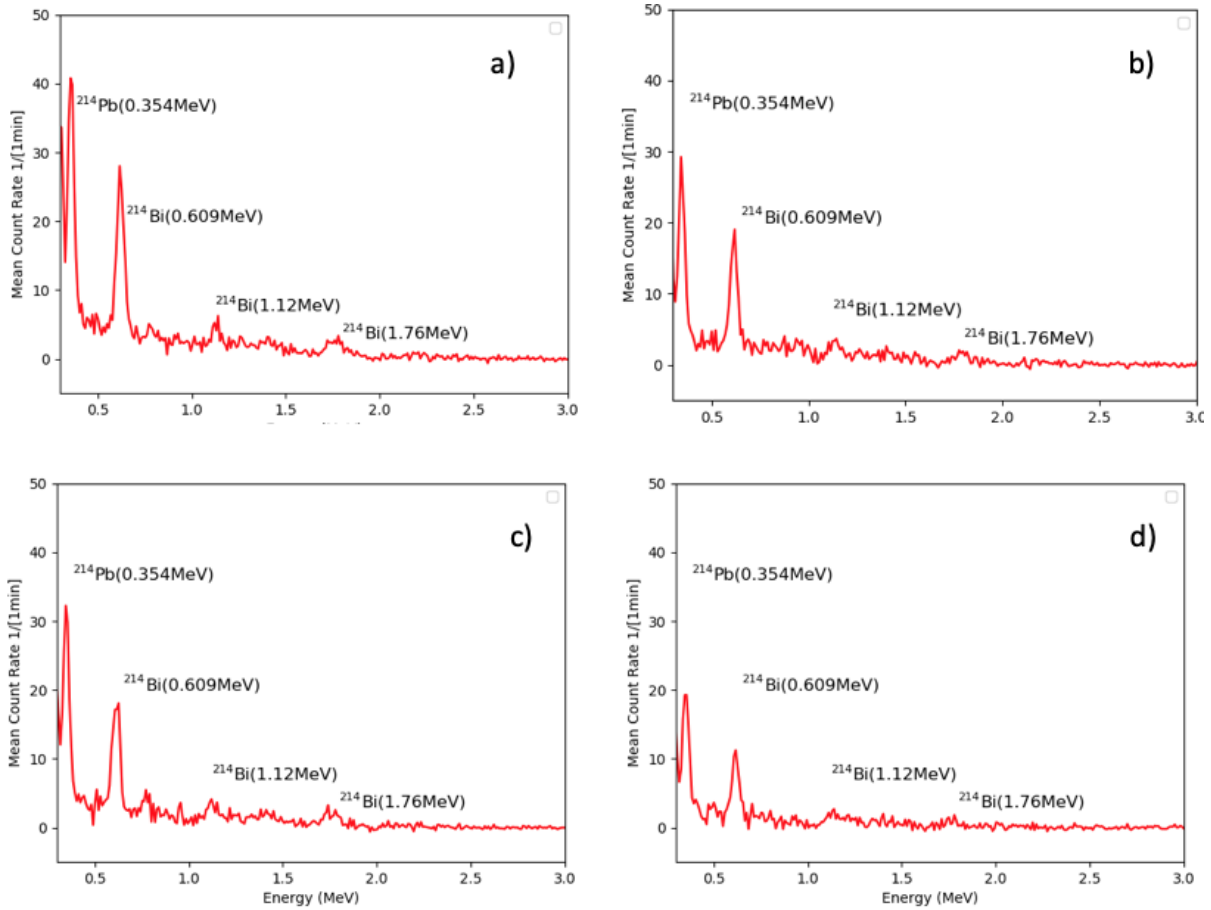


Figure 3. The Energy spectra of the rainwater measured by the ORTEC spectrometer covered by 4-cm thick lead filter from all sides: a) at 12:32 on 23 July ; b) at 18:27 on 23 July c) at 17:26 on 24 July; and d) at 14:16 on 1 August.

137
138

Table 2. Summary of the gamma radiation measurements from the rainwater by the ORTEC spectrometer covered by the 4-cm thick lead filter from all sides.

	Intensity 0.3 - 3 MeV	²¹⁴ Pb_ 354keV	511 keV	²¹⁴ Bi_ 609 keV	²¹⁴ Bi_ 768 keV	²²⁸ Ac_ 911 keV	²¹⁴ Bi_ 1.12 MeV	²¹⁴ Bi_ 1.76 MeV	²¹⁴ Bi_ 2.2 MeV	CR + Compton scattered
23 July Mean Count rate [12:32- 12:48] 1/min	585	147	5	109	45	26	40	32	7	174
%		25.1	0.9	18.6	7.7	4.4	6.8	5.5	1.2	29.7
23 July Mean Count rate [18:27 - 18:42] 1/min	531	123	6	102	32	43	38	23	8	156
%		23.2	1.1	19.2	6.0	8.1	7.2	4.3	1.5	29.4
24 July Mean Count rate [17:26 - 17:41] 1/min	814	191	8	161	46	41	60	42	12	253
%		23.4	1.0	19.7	5.7	5.0	7.4	5.2	1.5	31.1
01 Aug. Mean Count rate [14:16 - 14:31] 1/min	343	91	9	63	19	13	28	13	8	99
%		26.5	2.6	18.4	5.5	3.8	8.2	3.8	2.3	28.9
Mean %		24.6 ±1.5	1.4 ±0.8	19 ± 0.6	6.2 ± 1	5.3 ± 1.9	7.4 ± 0.6	4.7 ± 0.8	1.6 ± 0.5	29.8 ± 0.9

139
140
141
142

In Fig. 4 we present the decay curve of the most abundant ²¹⁴Pb isotope. The intensity was measured every 30 minutes for a period of 15 minutes and then normalized to the 1-minute count rate. Then the measured values were fitted with the exponential function and the half-life time calculated.

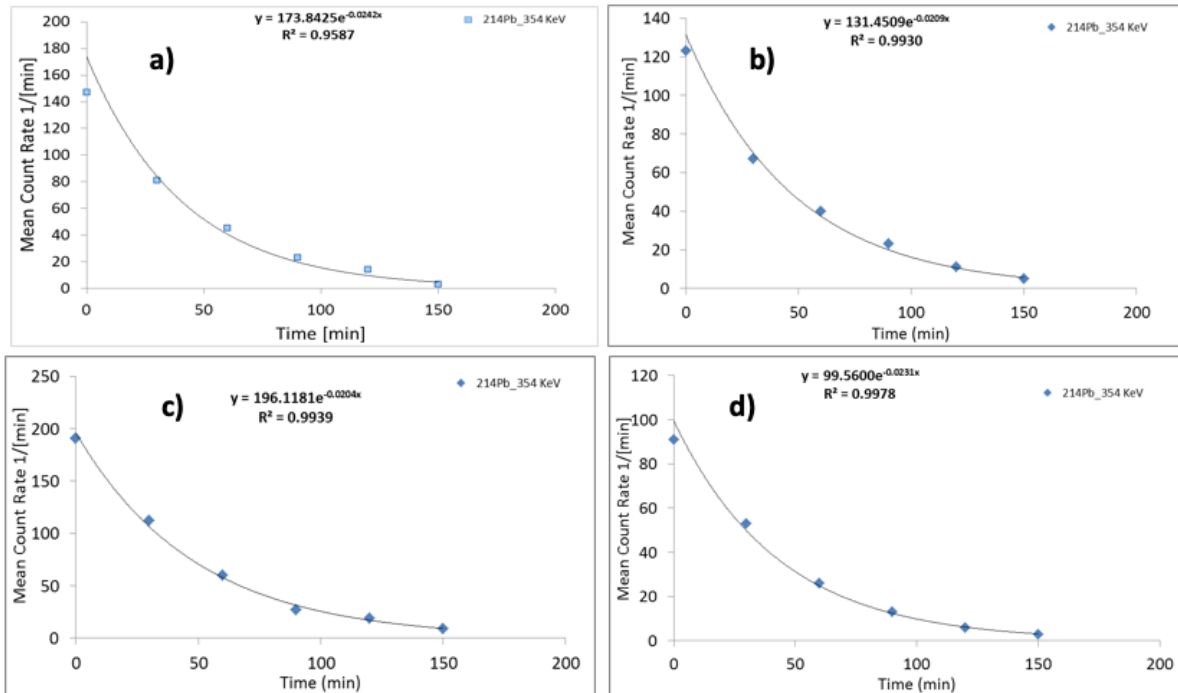


Figure 4. The exponential fit of the decay of the ^{214}Pb isotope. The intensity of the 354 keV line was measured each half-of-hour during 150 minutes of measurements. Solid line – the exponential fit.

The derived mean value of the ^{214}Pb (354 keV) isotope half-life time ($31.4 \pm 2.5\text{min}$) is larger than the real value of half-life time (26.8 min.). This shows that the collected rainwater contains the ^{222}Rn isotope and it continues to decay giving additional Pb-214 isotope, and in this way enlarging its half-life time. It means that rain washout not only gamma emitters (mostly Bismuth isotopes) but also ^{222}Rn itself.

4. Conclusions

We measured the gamma radiation of ^{222}Rn progeny during thunderstorms by precise gamma spectrometers located within the lead filter. The gamma radiation was measured from the rainwater collected during 4 summer storms on Aragats. The concentration of the most abundant gamma emitters in the rainwater ^{214}Pb , ^{214}Bi (609keV), ^{214}Bi (1.12 MeV) was $25.3 \pm 0.8\%$, $19.5 \pm 1\%$, and $7.5 \pm 0.2\%$ in the first minute of the exposing of the rainwater to the ORTEC spectrometer. In the last, 150-th minute of exposition, the concentration of these isotopes changed to $13.5 \pm 0.7\%$, $25.6 \pm 1.8\%$, and $17.1 \pm 2.8\%$ accordingly. The overall composition of the ^{222}Rn progeny in rainwater coincides well with one recovered from the registered gamma radiation of the atmospheric origin. Thus, near-surface electric field lifts the ^{222}Rn and its progeny up in the atmosphere and the rain return it backward in this way providing the circulation of the radioactive isotopes and enlarging surface radioactivity during thunderstorms.

ACKNOWLEDGMENTS

We thank the staff of the Aragats Space Environmental Center for safeguarding the operation of experimental facilities on Aragats. The data for this study is available on the WEB page of

170 the Cosmic Ray Division (CRD) of the Yerevan Physics Institute,
171 <http://adei.crd.yerphi.am/adei>.

172 **References**

173 Barbosa S.M., Miranda, P., Azevedo, E.B. (2017). Short-term variability of gamma radiation
174 at the ARM Eastern North Atlantic facility (Azores), Journal of Environmental Radioactivity
175 172, 218.

176
177 Chilingarian A. (2018). Long lasting low energy thunderstorm ground enhancements and
178 possible Rn-222 daughter isotopes contamination, Physical review D 98, 022007
179

180
181 Chilingarian, A., Avetisyan, A., Hovsepyan, G., et al. (2019a). Origin of the low-energy
182 gamma ray flux of the long-lasting thunderstorm ground enhancements, Phys. Rev. D 99,
183 102002.
184

185 Chilingarian, A., Hovsepyan, G., Elbekian, A., Karapetyan, T., Kozliner, L., Martoyan, H.,
186 Sargsyan, B. (2019b). Origin of enhanced gamma radiation in thunderclouds,
187 PhysRevResearch, **1**, 033167.

188 Chilingarian, M. Zazyan, G. Karapetyan (2019c). Modelling of the electron acceleration and
189 multiplication in the electric fields emerging in terrestrial atmosphere, Proceedings of the 8-th
190 TEPA symposium, Nor Amberd 2018, TIGRAN METS, 80.

191 Chilingarian, A., Hovsepyan, G., Karapetyan, T., et al., (2020). Structure of thunderstorm
192 ground enhancements, PRD 101, 122004.

193 Fabró, F., J. Montanyà, N. Pineda, et al. (2016). Analysis of energetic radiation asso-
194 ciated with thunderstorms in the Ebro delta region in Spain, J. Geo- phys. Res. Atmos., 121,
195 9879.

196 Hossain, I., Sharip, N., and Viswanathan, K.K. (2012). Efficiency and resolution of HPGe and
197 NaI(Tl) detectors using gamma- ray spectroscopy, Sci. Res. Essays 7, 86.

198 Hunting, E.R., Matthews J., Fernández de Arróyabe Hernáez, P. et al. (2020). Challenges in
199 coupling atmospheric electricity with biological systems, International Journal of
200 Biometeorology, <https://doi.org/10.1007/s00484-020-01960-7>.

201 Livesay, R.J., Blessinger, C.S., Guzzardo, T.F., Hausladen, P.A. (2014). Rain-induced
202 increase in background radiation detected by Radiation Portal Monitors, Journal of
203 Environmental Radioactivity 137, 137e14.

204 McCarthy, M., & Parks, G. K. (1992). On the modulation of X-ray fluxes in thunderstorms.
205 Journal of Geophysical Research, 97(D5), 5857–5864. <https://doi.org/10.1029/91JD03160>.

206

207 Reuveni Y., Yair Y., Price, c., and Steinitz, G., (2017). Ground level gamma-ray and electric
208 field enhancements during disturbed weather: Combined signatures from convective clouds,
209 lightning and rain, Atmospheric Research 196, 142–150.

210 Roffman, A. (1972). Short-lived daughter ions of radon-222 in relation to some atmospheric
211 processes, J. Geophys. Res., 27, 5883.

212 Sato, T. (2018). Analytical Model for Estimating the Zenith Angle Dependence of Terrestrial
213 Cosmic Ray Fluxes, PLOS ONE, 11(8): e0160390, <http://phits.jaea.go.jp/expacs/>.

214 Wilkcnig, M.H., Kawano M., and Lane, C. (1966). Radon-daughter ions and their relation
215 to some properties of the atmosphere, Tellus, 18, 679.

216

217

218

219

220

221

222

223